Journal of the Korean Nuclear Society
Volume 14, Number 2, June, 1982

《**Original**》

Plasma Rotation in Plasma Centrifuge with an Annular Gap

Hue Yeon Lee and Sang Hee Hong

Department of Nuclear Engineering, Seoul National University

(Received April 1, 1982)

동심 원통형 용기내에서의 플라즈마 회전

이 후 연 · 홍 상 희

서울대학교 원자핵공학과

(1982. 4. 1 접수)

Abstract

The steady-state rotation of plasma centrifuge is theoretically analyzed to understand the physics of rotating plasmas and its feasibility for isotope separation. The centrifuge system under consideration consists of an annular gap between coaxial cylindrical anode and cathode in the presence of an externally-applied axial magnetic field. A problem for coupled partial differential equations describing centrifuge fields is formulated on the basis of the magnetohydrodynamic equations. Two-dimensional solutions are found analytically in the form of Fourier-Bessel series. The current density and velocity distributions are discussed in terms of the Hartmann number and the geometrical parameter of the system. At typical conditions, rotational speeds of the plasma up to the order of 10^4m/sec are achievable, and increase either with increasing Hartmann number, or with increasing ratio of the axial length to the inner radius of the cylinder. In view of much higher speeds of rotation which can be achieved in plasma centrifuge, it is expected that its efficiency is superior to mechanically driven gas centrifuges.

요 약

정상상태의 플라즈마의 이론적 해석을 통해서 플라즈마의 회전과 동위원소 분리기로서의 적합성을 분석하였다. 이 장치는 두개의 동심원통형 전극과 이들 사이의 원통형 공동으로 구성되었으며, 축 방향으로 외부자장이 걸려 있다. 두 전극사이에 생성되는 전류밀도는 전기방전의 형태로 동위원소 혼합물로부터 플라즈마를 생성하고, 자장과 교차되어 발생하는 Lorentz힘에 의해서 플라즈마를 회전시킨다.

자기 유체역학 방정식을 바탕으로 이 계를 설명하는 두개의 연립편미분방정식을 얻었고, 네 경계조건을 사용하여 Fourier-Bessel로 표현된 이차원적 전류밀도와 속도분포의 해를 얻었다. 실제로 가능한 조건하에서 플라즈마 회전속도는 10^4m/sec 정도에 달하고, Hartmann수가 커짐에 따라 플라즈마회전 속도도 커진다. 이 같은 고속의 회전속도를 감안해 볼때 플라즈마 원심분리기는 기계적으로 회전되는 가스원심분리기보다 훨씬 높은 효율을 가지게 될 것이다.

I. Introduction

The plasma rotation by crossed electric and magnetic fields has been studied experimentally and theoretically with regard to applications as a plasma centrifuge for isotope separation.[1~15] In plasma centrifuges, the gaseous isotope mixture is brought into the plasma state through an electrical discharge. The plasma is set into rotation by Lorentz forces resulting from crossed current density and magnetic fields. The light and heavy ionic and atomic isotopes are spatially separated according to their masses. In contrast with mechanically driven conventional centrifuges, the plasma container is not subject to centrifugal stress and there is no maximum material strength limit of moving parts which imposes a limit on the achievable speeds of rotation. Thus, the plasma centrifuges using electromagnetic forces permit to generate high velocities unattainable in mechanical centrifuges. Plasma centrifuges have an additional advantage since they permit to control the driving forces by adjusting the current flow. The velocity profiles can then be optimized for the highest possible velocity at which stability is secured.

A theoretical work studied herein is mainly concerned with the steady-state dynamics of high-density plasma, which is confined in annular volume bounded by two perfectly-conducting coaxial cylindrical electrodes and two perfectly-insulating end closures. If an axial magnetic field is applied while a discharge current is being passed between the electrodes, an azimuthal Lorentz force causes the plasma to rotate. In general, the rotational motion of the plasma is retarded by viscous effects, and steady-state conditions are achieved when the momentum increase due to the Lorentz force is balanced by the frictional forces at the walls.

In order to reduce the magnetohydrodynamic equations describing centrifuge fields to a more tractable form, a number of simplifying assumptions must be made. All variables are assumed to be axially symmetric, and all physical properties of the plasma are assumed to be constant. The radial and axial components of velocity are to be small compared with the azimuthal component. Finally the radial current density at each electrode surface is to be constant. In this paper, two important centrifuge fields, azimuthal velocity and radial current density are found in dimensionless form in terms of the various dimensionless parameters. They indicate that extremely high speed of plasma rotation is obtainable at typical conditions that can be realized in practical applications of plasma centrifuges to isotope separation.

II. Model of Plasma Centrifuge

The plasma centrifuge shown in Fig. 1 consists of two coaxial cylindrical electrodes which are a perfectly conducting anode ($r=R_1$, $-c\leq z\leq c$) and a perfectly conducting cathode ($r=R_2$, $-c\leq z\leq c$). It is suggested that the cylindrical electrodes are placed very far from each other ($R_1 \ll R_2$), and the two insulating end walls ($z=$

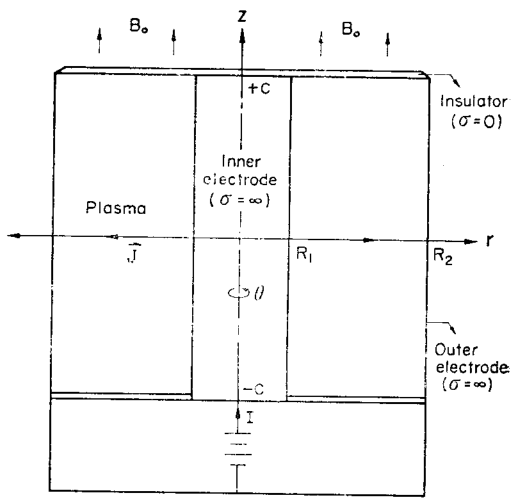

Fig. 1. Model of plasma centrifuge

$\pm c$, $R_1 \leq r \leq R_2$) are placed very far from each other ($R_1 \ll c$) to reduce velocity losses due to boundary layers at the electrodes and the end walls. The plasma is produced in the space $-c \leq z \leq c$, $R_1 \leq r \leq R_2$ through an electrical discharge in the gaseous isotope mixture between two cylindrical electrodes connected by an external source of current I. A current density distribution $J(r,z)$ intersects an axial external magnetic field B_0 in the annular volume. The resultant Lorentz force $J \times B_0$ rotates the charged isotope mixture with the velocity $V_\theta(r,z)$ around its axis of symmetry.

III. Theoretical Formulation and Analytical Solution

The steady-state rotation of the plasma centrifuge is theoretically investigated based on the magnetohydrodynamic equations for dense plasmas. In this model, laminar flow is assumed, and conceivable secondary flows superimposed on the main rotational flow are disregared. Some theoretical investigations indicate that the secondary flow in the motion of incompressible fluids in an annular gap is not occurred if their Reynolds number is not larger than a critical Reynolds number. In view of the symmetry of the centrifuge configuration with respect to z-axis, the plasma flow field is then azimuthal, $V = \{0, V_\theta(r,z), 0\}$, so that the plasma behaves incompressible ($\nabla \cdot V = 0$). It is assumed that the gyration frequency ω of the electrons is much smaller than the collision frequency τ^{-1} between electrons and neutral particles ($\omega\tau \ll 1$). It is generally accepted in partially ionized, collision-dominate, dense plasma. In this case, the current density is of the form $J = \{J_r(r,z), 0, J_z(r,z)\}$, and the Hall effect is negligible in the Ohm's law. The magnetic induction is of the form $B = \{0, B_\theta(r,z), B_0\}$ in accordance with Maxwell's equations and the homogeneous boundary conditions for B_r and B_z.

The plasma centrifuge is described by a boundary-value problem for the azimuthal velocity $V_\theta\ (r,z)$ and radial current density $J_r\ (r,z)$ field;

$$\frac{\partial}{\partial r}\left[\frac{1}{r}\frac{\partial}{\partial r}(rV_\theta)\right] + \frac{\partial^2 V_\theta}{\partial z^2} = \frac{B_0}{\mu} J_r \quad (1)$$

$$\frac{\partial}{\partial r}\left[\frac{1}{r}\frac{\partial}{\partial r}(rJ_r)\right] + \frac{\partial^2 J_r}{\partial z^2} = \sigma B_0 \frac{\partial^2 V_\theta}{\partial z^2} \quad (2)$$

where

$$V_\theta(r,z)\,|_{r=R_1,R_2} = 0, \quad -c \leq z \leq +c, \quad (3)$$

$$V_\theta(r,z)\,|_{z=\pm c} = 0, \quad R_1 \leq r \leq R_2 \quad (4)$$

and

$$J_r(r,z)\,|_{r=R_1,R_2} = \frac{I}{4\pi c R_{1,2}}, \quad -c \leq z \leq +c, \quad (5)$$

$$J_r(r,z)\,|_{z=\pm c} = 0, \quad R_1 \leq r \leq R_2. \quad (6)$$

Equations (1) and (2) are the azimuthal components of the equation of plasma motion and the induction equation combined with $\nabla \cdot J = 0$ and $\nabla \times B = \mu_0 J$, respectively. The boundary conditions (3) and (4) specify that the plasma does not slip at the chamber walls $r = R_1$, R_2 and $z = \pm c$. The boundary conditions (5) imply that a total discharge current I leaves uniformly the inner wire anode ($r = R_1$) and arrives uniformly at the outer cylindrical cathode wall ($r = R_2$). The boundary conditions (6) consider that no radial current flows at the end plates at $z = \pm c$ according to Ohm's law, $J_r = \sigma(E_r + V_\theta B_0)$, since $V_\theta(r,z)\,|_{z=\pm c} = 0$ and $E_r(r,z)\,|_{z=\pm c} = 0$ by $n \times [E] = 0$.

In order to solve analytically the boundary-value problem for the coupled plasma fields $V_\theta(r,z)$ and $J_r(r,z)$, it is convenient to formulate equations (1)~(6) in dimensionless form by introducing dimensionless variables,

$$\rho = r/R_1, \quad 1 \leq \rho \leq \rho_1, \quad \rho_1 \equiv R_2/R_1, \quad (7)$$

$$\zeta = z/c, \quad -1 \leq \zeta \leq +1, \quad (8)$$

and

$$V(\rho,\zeta) = V_\theta(r,z)/V_0, \quad j_\theta(\rho,\zeta) = J_r(r,z)/J_0, \quad (9)$$

where the reference values V_0 and J_0 are defined as

$$V_0 \equiv I/4\pi R_1 c B_0 \sigma,\ J_0 \equiv \sigma V_0 B_0 = I/4\pi R_1 c. \quad (10)$$

Thus, the boundary-value problem defined in equations (1)-(6) becomes for $V(\rho,\zeta)$ and $j_\rho(\rho,\zeta)$;

$$N^{-2}\frac{\partial^2 V}{\partial\zeta^2}+\frac{\partial}{\partial\rho}\left[\frac{1}{\rho}\frac{\partial}{\partial\rho}(\rho V)\right]=H^2 j_\rho, \quad (11)$$

$$N^{-2}\frac{\partial^2 j_\rho}{\partial\zeta^2}+\frac{\partial}{\partial\rho}\left[\frac{1}{\rho}\frac{\partial}{\partial\rho}(\rho j_\rho)\right] = N^{-2}\frac{\partial^2 V}{\partial\zeta^2}, \quad (12)$$

where

$$V(\rho,\zeta)\,|_{\rho=1,\,\rho_1}=0, \quad -1\leq\zeta\leq+1, \quad (13)$$

$$V(\rho,\zeta)\,|_{\zeta=\pm1}=0, \quad 1\leq\rho\leq\rho_1, \quad (14)$$

$$j_\rho(\rho,\zeta)\,|_{\rho=1,\,\rho_1}=\frac{1}{\rho}\,\Big|_{\rho=1,\,\rho_1}, \quad -1\leq\zeta\leq+1, \quad (15)$$

$$j_\rho(\rho,\zeta)\,|_{\zeta=\pm1}=0, \quad 1\leq\rho\leq\rho_1. \quad (16)$$

The dimensionless parameter N and H are defined by

$$N\equiv c/R_1, \quad H\equiv(\sigma/\mu)^{1/2}B_0R_1. \quad (17)$$

The Hartmann number H, which is a measure of the ratio of Lorentz force to viscous force. In general, one finds that as the Hartmann number is increased, a stabilizing effect of the magnetic field on the flow appears[16].

The general solutions of the coupled partial differential equations (11) and (12) are sought in the form of the Fourier-Bessel series;

$$V(\rho,\zeta)=-\frac{\pi^2}{2}\sum_n B_1(p_n\rho)\frac{p_n^2J_1^2(p_n\rho_1)}{J_1^2(p_n)-J_1^2(p_n\rho_1)}f_n(\zeta), \quad (18)$$

$$j_\rho(\rho,\zeta)=\frac{\pi^2}{2}\sum_n B_1(p_n\rho)\frac{p_n^2J_1^2(p_n\rho_1)}{J_1^2(p_n)-J_1^2(p_n\rho_1)}g_n(\zeta), \quad (19)$$

where $B_1(p_n\rho)=J_1(p_n\rho)Y_1(p_n)-Y_1(p_n\rho)J_1(p_n)$. (20)

$J_1(p_n\rho)$ and $Y_1(p_n\rho)$ are Bessel functions of the first order of the first and the second kinds, respectively. p_n is the n-th root of the transcendental equation

$$B_1(p_n\rho_1)=0. \quad (21)$$

Multiplying equations (11) and (12) by $\rho B_1(p_n\rho)$ and integrating with respect to ρ from 1 to ρ_1 with orthogonality condition for $B_1(p_n\rho)$, we get

$$\frac{\partial^2 f_n(\zeta)}{\partial\zeta^2}-N^2p_n^2f_n(\zeta)=N^2H^2g_n(\zeta), \quad (22)$$

$$\frac{\partial^2 g_n(\zeta)}{\partial\zeta^2}-N^2p_n^2g_n(\zeta)+\frac{2}{\pi}\left[j_\rho(\rho_1,\zeta)\frac{J_1(p_n)}{J_1(p_n\rho_1)}-j_\rho(1,\zeta)\right]N^2=\frac{\partial^2 f_n(\zeta)}{\partial\zeta^2}, \quad (23)$$

and the the boundary conditions;

$$f_n(\zeta)\,|_{\zeta=\pm1}=0, \quad (24)$$

$$g_n(\zeta)\,|_{\zeta=\pm1}=0. \quad (25)$$

By elimination, equations (22) and (23) are reduced to decoupled differential equations of fourth order,

$$f_n''''-N^2(2p_n^2+H^2)f_n''+N^4p_n^4f_n=-H^2N^4\alpha_n \quad (26)$$

$$g_n''''-N^2(2p_n^2+H^2)g_n''+N^4p_n^4g_n=p_n^2N^4\alpha_n \quad (27)$$

where

$$\alpha_n=\frac{2}{\pi}\left[\frac{J_1(p_n)}{\rho_1J_1(p_n\rho_1)}-1\right]. \quad (28)$$

$f_n(\zeta)$ and $g_n(\zeta)$ have to satisfy also the coupled equations (22) and (23). The general solutions for $f_n(\zeta)$ and $g_n(\zeta)$ of equations (26) and (27) can be written as

$$f_n(\zeta)=A_n^+\frac{\sinh(w_n^+\zeta)}{\sinh(w_n^+)}+B_n^+\frac{\cosh(w_n^+\zeta)}{\cosh(w_n^+)}+A_n^-\frac{\sinh(w_n^-\zeta)}{\sinh(w_n^-)}+B_n^-\frac{\cosh(w_n^-\zeta)}{\cosh(w_n^-)}-\frac{H^2\alpha_n}{p_n^4}, \quad (29)$$

$$g_n(\zeta)=C_n^+\frac{\sinh(w_n^+\zeta)}{\sinh(w_n^+)}+D_n^+\frac{\cosh(w_n^+\zeta)}{\cosh(w_n^+)}+C_n^-\frac{\sinh(w_n^-\zeta)}{\sinh(w_n^-)}+D_n^-\frac{\cosh(w_n^-\zeta)}{\cosh(w_n^-)}+\frac{\alpha_n}{p_n^2}. \quad (30)$$

Four real roots of the characteristic equations of homogeneous parts of equations (26) and (27) are given by

$$\pm w_n^\pm=\pm\tfrac{1}{2}N\{(H^2+4p_n^2)^{1/2}\pm H\}. \quad (31)$$

Only four of the eight integration constants

$A_n^{\pm}$, $B_n^{\pm}$, $C_n^{\pm}$, $D_n^{\pm}$, are independent. Substitution of equations (29) and (30) into equations (22) and (23) yields

$$A_n^{\pm}[(w_n^{\pm})^2-p_n^2N^2]=H^2N^2C_n^{\pm},$$
$$B_n^{\pm}[(w_n^{\pm})^2-p_n^2N^2]=H^2N^2D_n^{\pm},$$
$$C_n^{\pm}[(w_n^{\pm})^2-p_n^2N^2]=(w_n^{\pm})^2A_n^{\pm},$$
$$D_n^{\pm}[(w_n^{\pm})^2-p_n^2N^2]=(w_n^{\pm})^2B_n^{\pm}, \quad (32)$$

respectively. For the condition for existence of nontrivial solution, the coefficient determinant of equation (32) vanishes

$$\Delta^{\pm}=[(w_n^{\pm})^2-p_n^2N^2]^2-(w_n^{\pm})^2H^2N^2=0 \quad (33)$$

in agreement with equation (31). From the latter or equation (33) one deduces the relations,

$$(w_n^{\pm})^2-p_n^2N^2=\pm HNw_n^{\pm}, \quad (34)$$

which simplify equations (32). Application of the boundary conditions (24) and (25) to equations (29) and (30) and use of the relations (32) yield

$$A_n^{\pm}=0,\ C_n^{\pm}=0,$$
$$B_n^{\pm}=\frac{HN\alpha_n}{p_n^2(w_n^++w_n^-)}\left[\frac{Hw_n^{\mp}}{Np_n^2}\mp1\right],$$
$$D_n^{\pm}=\frac{\pm\alpha_n w_n^{\pm}}{p_n^2(w_n^++w_n^-)}\left[\frac{Hw_n^{\mp}}{Np_n^2}\mp1\right]. \quad (35)$$

By combing equations (29) and (30) with equations (35) the solutions for $f_n(\zeta)$ and $g_n(\zeta)$ in final form are

$$f_n(\zeta)=\frac{2}{\pi p_n^2}\left[\frac{J_1(p_n)}{\rho_1J_1(p_n\rho_1)}-1\right]\left[\frac{HN}{(w_n^++w_n^-)}\left\{\left(\frac{Hw_n^-}{Np_n^2}-1\right)\frac{\cosh(w_n^+\zeta)}{\cosh(w_n^+)}+\left(\frac{Hw_n^+}{Np_n^2}+1\right)\frac{\cosh(w_n^-\zeta)}{\cosh(w_n^-)}\right\}-\frac{H^2}{p_n^2}\right], \quad (36)$$

$$g_n(\zeta)=\frac{2}{\pi p_n^2}\left[\frac{J_1(p_n)}{\rho_1J_1(p_n\rho_1)}-1\right]\left[\frac{1}{(w_n^++w_n^-)}\left\{w_n^+\left(\frac{Hw_n^-}{Np_n^2}-1\right)\frac{\cosh(w_n^+\zeta)}{\cosh(w_n^+)}-w_n^-\left(\frac{Hw_n^+}{Np_n^2}+1\right)\frac{\cosh(w_n^-\zeta)}{\cosh(w_n^-)}\right\}+1\right]. \quad (37)$$

In terms of $f_n(\zeta)$ and $g_n(\zeta)$, the solutions for the dimensionless fields V and j_ρ of the plasma centrifuge are by equations (18) and (19)

$$V(\rho,\zeta)=\frac{\pi^2}{2}\sum_n B_1(p_n\rho)\frac{p_n^2J_1^2(p_n\rho_1)}{J_1^2(p_n)-J_1^2(p_n\rho_1)}f_n(\zeta), \quad (38)$$

$$j_\rho(\rho,\zeta)=\frac{\pi^2}{2}\sum_n B_1(p_n\rho)\frac{p_n^2J_1^2(p_n\rho_1)}{J_1^2(p_n)-J_1^2(p_n\rho_1)}g_n(\zeta). \quad (39)$$

In the case that the axial length 2c is much larger than the distance R_2-R_1 between the inner and outer cylindrical electrodes, the plasma centrifuge fields V and J do not depend on z[17]. This system is described by the following dimensionless equations and the boundary conditions;

$$\frac{\partial}{\partial\rho}\left[\frac{1}{\rho}\frac{\partial}{\partial\rho}(\rho V)\right]=H^2j_\rho, \quad (40)$$

$$\frac{\partial}{\partial\rho}\left[\frac{1}{\rho}\frac{\partial}{\partial\rho}(\rho j_\rho)\right]=0, \quad (41)$$

and

$$V(\rho)\,|_{\rho=1,\rho_1}=0, \quad (42)$$

$$j_\rho(\rho)\,|_{\rho=1,\rho_1}=0, \quad (43)$$

which are equivalent to equations (11)-(16) for $N\to\infty$.

The plasma centrifuge fields V and j_ρ for a boundary-value problem give by equations (40) and (43) have the simple solutions;

$$V(\rho)=\frac{H}{2}\left[\rho\ln\rho-\frac{\rho_1^2\ln\rho_1}{\rho_1^2-1}\rho(\rho-\rho^{-2})\right], \quad (44)$$

$$j_\rho(\rho)=\rho^{-1}. \quad (45)$$

It can be shown that as $N\to\infty\,(w_n^{\pm}\to\infty)$, solutions (38) and (39) for the plasma centrifuge with finite axial length are transformed into solutions (44) and (45) for that with quasi-infinite axial length by using the following Fourier-Bessel series[18];

$$\frac{1}{\rho}=\pi\sum_n B_1(p_n\rho)\left[\frac{J_1(p_n\rho_1)}{J_1^2(p_n)-J_1^2(p_n\rho_1)}\right]\left[\frac{J_1(p_n)}{\rho J_1(p_n\rho_1)}-1\right], \quad (46)$$

$$\rho(1-\rho^{-2})\frac{\rho_1^2\ln\rho_1}{\rho_1^2-1}-\rho\ln\rho=2\pi\sum_n B_1(p_n\rho)p_n^{-2}\left[\frac{J_1^2(p_n\rho_1)}{J_1^2(p_n)-J_1^2(p_n\rho_1)}\right]\left[\frac{J_1(p_n)}{\rho_1J_1(p_n\rho_1)}-1\right]. \quad (47)$$

IV. Discussion and Result

As numerical illustrations, the axial (ζ) and radial (ρ) dependences of the dimensionless centrifuge fields $V(\rho, \zeta)$ and $j_\rho(\rho, \zeta)$ have been calculated in some interesting cylindrical region ($\rho=2.5$) and cross-sectional plane ($\zeta=0$), respectively. Since the centrifuge fields $V(\rho, \zeta)$ and $j_\rho(\rho, \zeta)$ depend only on ρ_1, N and H, the Hartmann numbers are treated as parameters,

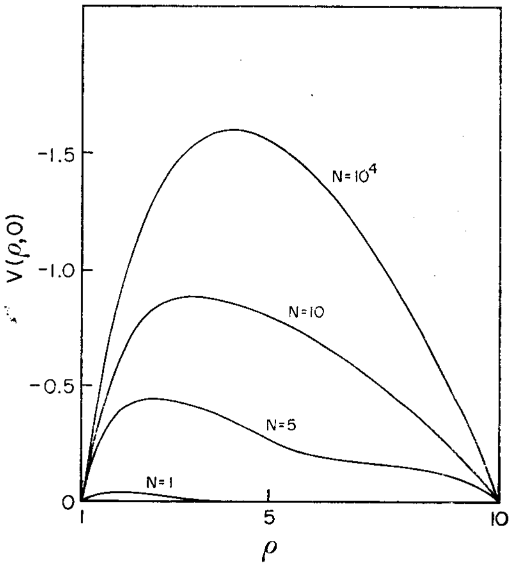

Fig. 2. $V(\rho, 0)$ **versus** ρ **for** $\rho_1=10$, $H=1$, $N=$ **1.5, 10,** 10^4.

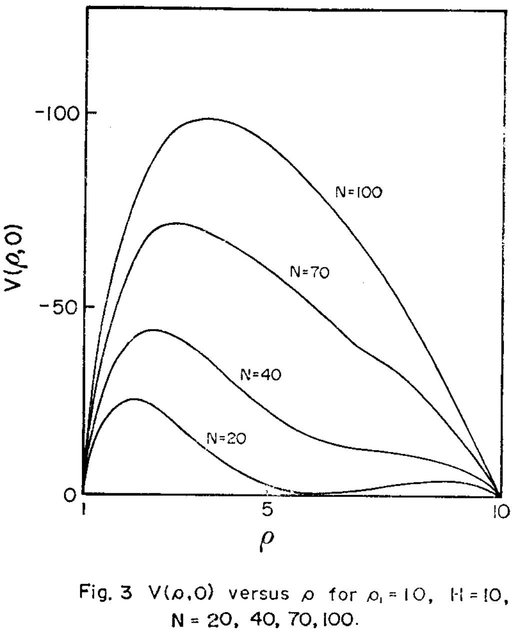

Fig. 3. $V(\rho, 0)$ **versus** ρ **for** $\rho_1=10$, $H=10$, $N=$ **20, 40, 70, 100.**

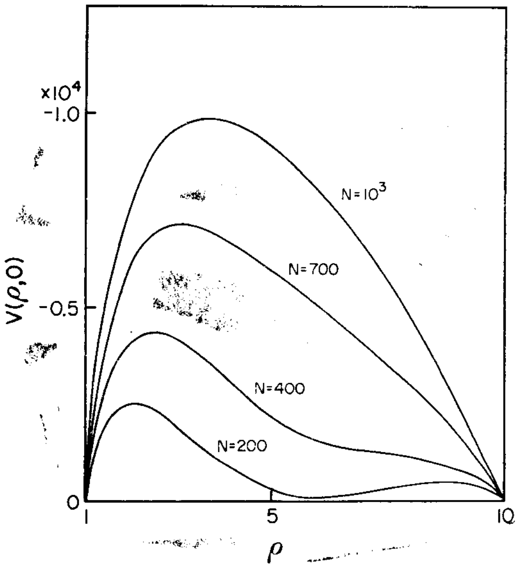

Fig. 4. $V(\rho, 0)$ **versus** ρ **for** $\rho_1=10$, $H=100$, $N=$ **2, 4, 7,** 10×10^2.

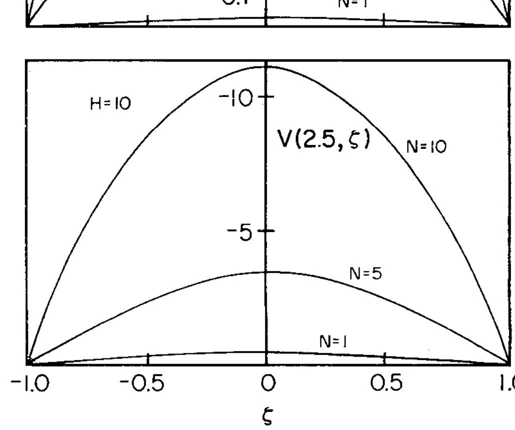

Fig. 5. $V=(2.5, \zeta)$ **versus** ζ **for** $\rho_1=10$, $H=1, 10$, $N=1, 5, 10$.

$H=1$, 10, 100. The geometry parameters are taken as $\rho_1=R_2/R_1=10$, and $N=c/R_1=1, 5, 10, 10^4$ for $H=1$; $N=20$, 40, 70, 100 for $H=10$; and $N=2, 4, 7, 10\times 10^2$ for $H=100$. The radial positions of the anode and cathode are at $\rho=1$ and $\rho=\rho_1$, respectively. The solutions in equations (36)-(39) indicate that $V(\rho, \zeta)$ and $j_\rho(\rho, \zeta)$ and $j_\rho(\rho, \zeta)$ are symmetric with respect to the central planes ($\zeta=0$).

Velocity fields $V(\rho, \zeta)$ [Fig. 2~Fig. 5]: The azimuthal velocity fields are symmetric about $\zeta=0$ and are distributed over the entire system, $1<\rho<\rho_1$, $|\zeta|<1$, with zero velocity at end walls and surface of electrodes. The maxima of $|V|$ are at the central planes ($\zeta=0$) and move toward the anode wall ($\rho=1$) as H is increased or N is decreased. It is also observed that $|V|$ stretches along and dwindles at any point $0<\rho<1$ as N is reduced. At large N velocity is proportional to the square of the Hartmann number by equation (48).

Current density fields $j_\rho(\rho, \zeta)$ [Fig. 6 and Fig. 7]: The electric descharges become more closely concentrated near the electrode walls as H is increased or N is decreased. In the middle

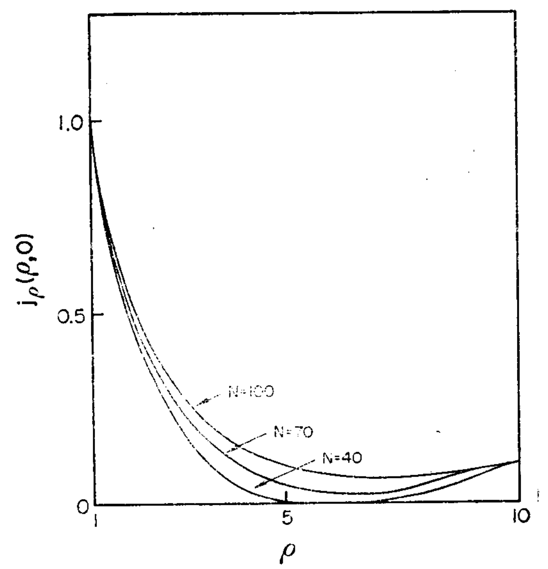

Fig. 6. $j_\rho(\rho, 0)$ **versus** ρ **for** $\rho_1=10$, $H=10$, $N=40, 70, 100$.

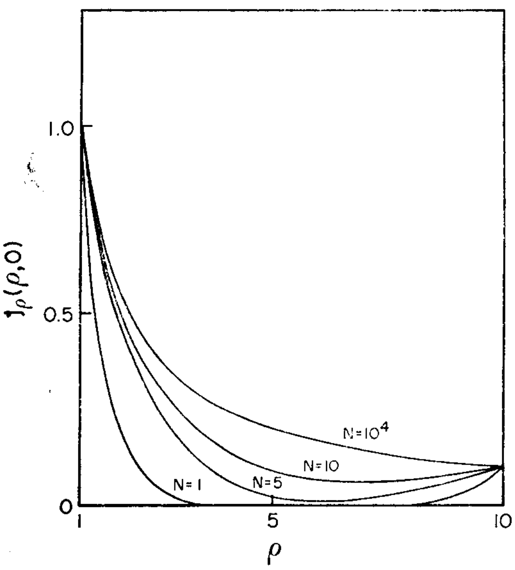

Fig. 7. $j_\rho(\rho, 0)$ **versus** ρ **for** $\rho_1=10$, $H=1$, $N=1, 5, 10, 10^4$.

region the current density is smaller than other region near electrodes, and is decreased as N is decreased.

The graphical presentation of the plasma fields indicates that it is desirable for the column length to be much larger than the distance between anode and cathode ($N=c/R_1\gg 1$ at the same ρ_1). It ensures in this case that a significant Lorentz force and plasma rotation, and that velocity losses due to boundary layers at end walls are insignificant. The proposed centrifuge scheme results in supersonic rotational plasma velocities for moderate flow numbers H, N, ρ_1 that are realizable in practical applications. For example, in the case that $I=10^2$ amp, $B_0=1$ tesla, $\sigma=10^2$mho/m and $\rho_1=10$, $R_1=0.5$cm, we get $V_0=I/4\pi R_1^2 N B_0=31.8$m/sec by Eq. (10), $V=2\times 10^3$ from Fig. 4 for $H=100$ and $N=100$. The speed of plasma rotation is thus 10^4m/sec in order of magnitude in typical conditions of the plasma centrifuge.

Either the larger Hartmann number becomes or the smaller R_1 becomes, the higher the rotational velocity is achieved. But the anode is limited to have considerable radius since the high currents pass through the anode. The associated centrifugal forces produce a significant spatial isotope separation. In view of much higher speeds of rotation which can be achieved in plasma centrifuge, it is expected that its efficiency is superior to mechanically-driven gas centrifuges.

REFERENCES

1. D.V. Berezov, I.I. Demidenko, N.S. Lomino, and A.I. Morozov, *Sov. Phys. Tech. Phys.* **20**, 906 (1976).
2. A.V. Belorusov, A.I. Karchevskii, and E.P. Pontanin, *Pisma V. Zh. Tekh. Fiz.* 12, 664 (1976).
3. B. Bonnevier, *Ark. Fys.* 33, 255 (1966).
4. B. Bonnevier, *Plasma Phys.* 13, 763 (1971).
5. B. Lehnert, *Phys. Scrip.* 2, 106 (1970).
6. B. Lehnert, *Nucl. Fusion* **11**, 485 (1971).
7. B. Lehnert, *Phys. Scrip.* 7, 102 (1973).
8. O. Okada, T. Dodo, and T. Kawai, *J. Nucl. Sci. Tech.* **10**, 626 (1973).
9. D.W. George and E.L. Kane, *IEE* **90**, 174 (1972).
10. B.W. James and S.W. Simpson, *Phys. Lett.* **46A**, 347 (1974).
11. B.W. James and S.W. Simpson, *Plasma Phys.* **18**, 289 (1976).
12. H. Heller and M. Simon, *Phys. Lett.* **50A**, 139 (1974).
13. S.H. Hong and H.E. Wilhelm, *J. Appl. Phys.* **49**, 146 (1978).
14. H.E. Wilhelm and S.H. Hong, *Phys. Rev.* **15**, 2108 (1977).
15. H.E. Wilhelm and S.H. Hong, *J. Appl. Phys.* **48**, 561 (1977).
16. S.H. Hong and H.E. Wilhelm, *J. Appl. Phys.* **47**, 906 (1976).
17. G.V. Gordeev and A.I. Gubanov, *Sov. Phys. Tech. Phys.* 3, 1880 (1958).
18. G.N. Watson, "Theory of Bessel Function,' Cambridge University Press, Cambridge (1966).